Agri. & Biosys. Eng. Vol. 6(2):39-46(2005)

On-the-go Soil Strength Profile Sensor to Quantify Spatial and Vertical Variations in Soil Strength

S. O. Chung, K. A. Sudduth

Abstract: Because soil compaction is a concern in crop production and environmental pollution, quantification and management of spatial and vertical variability in soil compaction (or soil strength) would be a useful aspect of site-specific field management. In this paper, a soil strength profile sensor (SSPS) that could take measurements continuously while traveling across the field was developed and the performance was evaluated through laboratory and field tests. The SSPS obtained data simultaneously at 5 evenly spaced depths up to 50 cm using an array of load cells, each of which was interfaced with a soil-cutting tip. Means of soil strength measurements collected in adjacent, parallel transects were not significantly different, confirming the repeatability of soil strength sensing with the SSPS. Maps created with sensor data showed spatial and vertical variability in soil strength. Depth to the restrictive layer was different for different field locations, and only 5 to 16% of the tested field areas were highly compacted.

Keywords: Precision Agriculture, Soil Sensor, Soil Strength, Soil Compaction

Introduction

Site-specific crop management (SSCM) has been studied and increasingly adopted in many countries throughout the world. Soil properties are some of the most important information sources for SSCM because soil physical and chemical properties govern the transport of nutrients and water in the soil and the amount of plant available nutrients and water (Barber, 1984). Compaction, a soil physical property, is a concern in crop production and environmental pollution. Soil compaction often restricts root development and growth (Lipiec and Stepniewski, 1995) due to increased bulk density and/or strength of the soil (Guerif, 1994), reduces the biological activity of plant roots and organisms in the soil due to reduced aeration (Voorhees et al., 1975), and limits water infiltration. The causes of soil compaction and the resulting soil deformations may be different in the various soil layers (i.e., top layer, arable layer, and subsoil) (Koolen and Kuipers, 1983). Therefore, quantifying spatial and vertical variability in soil compaction and related soil properties would be useful in SSCM.

The authors are **Sun-Ok Chung**, Agricultural Engineering Researcher, National Institute of Agricultural Engineering, Suwon, Republic of KOREA; and **Kenneth A. Sudduth**, Agricultural Engineer, USDA-ARS Cropping Systems and Water Quality Research Unit, University of Missouri, Columbia, Missouri, USA. **Corresponding author:** Sun-Ok Chung, National Institute of Agricultural Engineering, Rural Development Administration, 249 Seodun-dong Kwonsun-gu, Suwon, 441-707, Republic of KOREA; e-mail: sochung@rda.go.kr

The degree of soil compaction, called compactness, traditionally has been determined through laboratory tests of soil samples and expressed as pore space, void ratio, or bulk density (Koolen and Kuipers, 1983). An alternative approach to estimate the state of soil compaction is to measure soil strength, since soil strength is strongly associated with compactness, packing density, relative bulk density, and drainable porosity (Canarache, 1991). Laboratory determination of either soil compactness or soil strength at the spatial resolution needed in SSCM is time-consuming, laborious, and expensive even if the required, spatially-dense sampling is possible.

To overcome the limitations of laboratory tests, field sensors such as cone penetrometers (Mulqueen et al., 1977) have been developed to quantify soil properties related to soil compaction or soil strength. The index of soil strength measured by a cone penetrometer, cone index (CI), is defined as the force per unit base area required to push the penetrometer through a specified small increment of soil depth (ASAE, 2003a; ASAE, 2003b). Cone penetrometer readings require a "stop-and-go" procedure and only collect data at discrete locations, making it difficult to collect the amount of data required for SSCM. Even in nonspatial analyses, researchers have often collected hundreds of penetrometer readings to investigate treatment differences (Busscher et al., 1986) and to relate cone index to soil properties such as water content and bulk density (Sojka et al., 2001).

To improve data collection efficiency, a number of researchers have attempted "on-the-go" measurement of soil strength. These approaches have differed in : (1) the type of soil strength measured: tillage draft (e.g., Van Bergeijk et al., 2001), bending stress on a tine (e.g., Adamchuk et al., 2001), and "CI-like" soil resistance experienced by a soil-penetrating tip (e.g., Andrade et al., 2001), (2) the number of sensing elements: single (e.g., Alihamsyah et al., 1990) and multiple (e.g., Chukwu and Bowers, 2005), and (3) the shape and extension of sensing tips: 30° conical extended tip (Alihamsyah et al., 1990) and 30° prismatic flush-mounted tip (e.g., Hall and Raper, 2005). Although these prototype sensors have been able to provide on-the-go soil strength data, they are all still in development and testing stages. Advantages and disadvantages have been reported for each approach, and additional efforts in sensor development are warranted to obtain "CI-like" measurements with a soil-penetrating tip in an efficient manner. Testing such a sensor under various soil and operating conditions is necessary for better interpretation of the sensor measurements and developing applications for sensor data.

The objectives of the research were (1) to develop an on-the-go soil strength profile sensor (SSPS) that could take measurements continuously while traveling across the field and simultaneously at multiple depths, and (2) to evaluate the performance through laboratory and field tests.

Materials and Methods

1. Design and Fabrication

The SSPS design concept enabled measurement of soil strength at multiple depths (fig. 1). Each force-sensing tip interfaced with a load cell located inside a narrow soil-cutting blade and was extended in front of the blade edge. The main blade was mounted to a frame using a shear bolt mechanism and the frame was attached to a tractor 3-point hitch. Major design issues were (1) soil strength sensing, (2) data acquisition and calibration, (3) selection of materials for the main blade and sensing tip, and (4) tractor attachment and overload protection. Results obtained from our previous work in preliminary data analysis and soil failure modeling were used as guidelines for sensor design :

- Maximum sensing depth, expected maximum soil strength, and sensing resolution were selected as 50 cm, 10 MPa, and 0.1 MPa, respectively, based on examination of CI profiles from a Missouri claypan soil field (Chung and Sudduth, 2004). Higher loads due to dynamic operation of the sensor, along with a safety factor, were considered for appropriate load cell selection and sensor design. The desired maximum vertical sensing interval was 10 cm, contingent on being able to obtain accurate strength data from tips on that spacing.

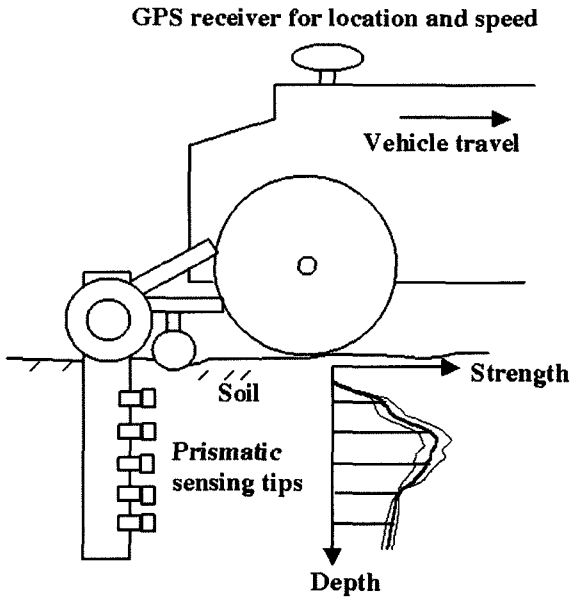

Fig. 1 Operational concept of the on-the-go soil strength profile sensor.

- High-resolution and high-frequency data acquisition was needed to capture variability in soil strength. Assuming a 2-m s^{-1} normal operating speed, a minimum sampling frequency of 4 Hz was selected to detect repeating spatial patterns in CI (e.g., wheel traffic patterns). Faster data acquisition would be desirable for more reliable measurements and would allow application of filtering techniques such as a moving average (Chung and Sudduth, 2004).

- A prismatic tip with a 60° cutting or apex angle was selected as the sensing tool to reduce soil disturbance and avoid extreme force measurements for most soils, based on modeling and simulation of soil failure mechanisms (Chung and Sudduth, 2003).

Load cells and materials for the main blade and prismatic tip were selected based on the expected maximum soil strength (10 MPa) and a material analysis. A miniaturized circular load cell with a diameter of 12.7 mm (Model 8402, Burster GMBH, Gernsbach, Germany[1]) was selected. The sensor had a full bridge circuit of foil strain

gauges with temperature compensation from 15℃ to 70℃. Static capacity, dynamic capacity, and accuracy of the load cell were 0 to 10 kN, 0 to 7 kN, and better than 50 N (0.5% of full scale), respectively. Force data for each tip were processed in parallel through a series of data acquisition components. The output of the Burster 8402 load cell was 1.5 mV V^{-1} at rated load (10 kN). A 3-V excitation input was used, resulting in a 4.5-mV signal at 10 kN. The signal from each load cell was sent to a data acquisition system (DaqBook/100, Iotech Inc., Cleveland, Ohio) through a transducer amplifier (Model S7DC, RDP Electrosense Inc., Pottstown, Pa.). The amplifier provided a variable gain, which was set at its maximum value of 1,250 for this application, and low-pass filtering with a 20-Hz bandwidth. The data acquisition system had a 100-kHz, 12-bit, 16-channel, 10-V A/D converter and a programmable gain setting function (set at a value of 2 for this application). Data from the DaqBook/100 was transmitted to a laptop computer through the parallel port. During field data collection, position information was obtained simultaneously from a DGPS receiver (approximately 1-m accuracy) through the computer's serial port. Using manufacturer's specifications, the output of the data acquisition system (as a digital number, DN) was transformed to a theoretical force (kN):

$$Force(kN) = \frac{DN}{R_{da} \times G_{da} \times G_{lc} \times V_{in}} = 2.17 \times 10^{-3} DN \quad (1)$$

where R_{da} = data acquisition system resolution, 4096 counts $(10\ V)^{-1}$

G_{da} = data acquisition system gain, 2500

G_{lc} = load cell gain, 1.5×10^{-3} V V^{-1} $(10\ kN)^{-1}$

V_{in} = load cell input voltage, 3 V

To allow more direct comparison with the CI of a cone penetrometer, we defined a prismatic soil strength index (PSSI, MPa) as the force measured by the SSPS divided by the base area of the prismatic tip:

$$PSSI(MPa) = \frac{Force(kN) \times 10^{-3}}{A_{tip}} = 2.77 \times Force(kN) = 6.01 \times 10^{-3} DN \quad (2)$$

where A_{tip} = projected area of sensing tip, 3.61×10^{-4} m^2

[1] Mention of trade names or commercial products is solely for the purpose of providing specific information and does not imply recommendation or endorsement by NIAE, Korea or USDA-ARS, USA.

The main blade had a cutting angle of 60° and consisted of body and cover plates of stainless steel (86×18 cm, AISI No. 17-4PH). The body plate was machined to create pockets for the load cells, wiring tunnels, and grooves for the prismatic tips. To create each prismatic tip, one end of a square stainless steel (AISI No. 304) bar with a 361 mm^2 cross-section was machined to an apex angle of 60° (fig. 2, left). The prismatic tips were extended 5.1 cm in front of the SSPS blade and spaced 10 cm apart to minimize effects of the blade and adjacent tips on the force measurements. The main blade was mounted to a frame using a shear bolt mechanism, and the frame was attached to a tractor 3-point hitch (fig. 2, right). Additional details of the SSPS design are given in Chung (2004).

2. Senor Optimization and Improvement

Preliminary field tests were conducted to verify the performance of the sensor and to determine if modifications were needed to enhance the reliability of the sensor under field conditions. The main concerns addressed in these tests were electrical noise from the environment, overload in the case of excessive soil resistance, and penetration of the sensor into the soil.

The sensor was susceptible to radio frequency interference (RFI) and the main blade acted as an antenna, picking up signals from a local television station (broadcast antenna within 1 km). Based on field tests, an aluminum shield was fabricated for the above-ground portion of the sensor, and reduced RFI to acceptable levels (Chung, 2004). Addi-

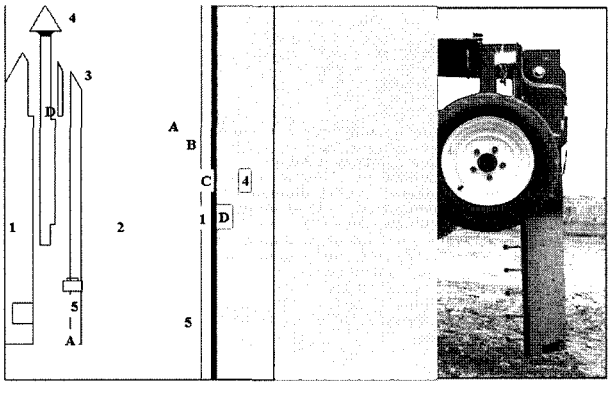

Fig. 2 Structure of the main blade (not to scale, left) and side view of the SSPS raised out of the ground (right). Components include body plate (1), cover plate (2), retaining bar (3), prismatic tip with 1.9×1.9 cm base area (4), and load cell (5). Parts of the body plate include wiring tunnel (A), holes for load cells (B), grooves for prismatic tips (C) and groove for retaining bar (D).

tionally, we discovered that a major portion of the noise occurred only when the sensor and the mounting frame were oriented in a certain direction relative to the broadcast antenna. Therefore, care was taken to avoid this orientation for subsequent data collection at the test site.

As initially designed, the sensor relied on an aggressive suction foot for penetration; however this caused the shear bolt to fail repeatedly in high-strength soil conditions. After several modifications (Chung, 2004), a configuration that provided acceptable penetration without draft force overloads was attained. This revised configuration included (1) a less aggressive 30°-rake angled, 3.8×7.6 cm suction foot, a revised main blade with the overall length reduced to 57 cm and the lower edge angled backward approximately 10° to reduce the surface area of the blade bottom in contact with the soil, and (3) the addition of approximately 180 kg of weight to the sensor mounting frame. With these revisions, the sensor could penetrate to the full operating depth (i.e., 0.5 m) after 3 to 5 m of forward travel.

3. Experimental Design and Data Analysis

Laboratory tests were conducted (1) to verify performance of the selected load cells, and (2) to verify equations 1 and 2 by testing the output of each amplifier with known forces. A cylindrical laboratory test fixture with three equally spaced holes smoothly fitting to the load cells was fabricated. Initially a cylindrical metal plate was put on top of the load cells and the zero-offset of the data acquisition system was adjusted. Then, five tractor weights were loaded and unloaded one by one. Forces applied by the weights were 0, 0.32, 0.66, 0.99, 1.32, and 1.64 kN. At each loading and unloading increment, each of the three load cells in the fixture was connected to all five of the amplifiers one by one and the amplified load cell signal output was sampled at a 100-Hz rate for 20 s. In this way, the signals representing the total, known weight at each stage were routed through each amplifier and the resulting output recorded. Accurate testing was not possible by merely pairing an individual amplifier with each load cell because the fraction of the calibration weight supported by each of the three load cells in the fixture was unknown and not likely to be equal.

The distribution of each output was examined to verify the stability of the load cell signal. For amplifier calibration, the total response of each amplifier was obtained by summing outputs from the three load cells for each loading stage, which resulted in six data points for each amplifier, corresponding to the six loading levels listed above. The REG procedure in SAS version 8.01 (SAS Institute Inc., Cary, N.C.) was used to obtain a linear relationship between measured digital number and applied force.

Field data were collected to verify (1) the capability of the SSPS to detect spatial and vertical within-field variability in PSSI and (2) the stability and repeatability of PSSI measurements. Field data was collected at two research sites. The sites were chosen based on knowledge obtained from previous research (e.g., Sudduth et al., 2003), along with consideration of spatial patterns of apparent soil electrical conductivity (EC_a) measured with a Veris Model 3100 sensor. The claypan soils found at site 1 (13.5 ha) were relatively fine textured, while the alluvial soils at site 2 (4.5 ha) in the Missouri River flood plain were relatively coarse textured.

PSSI data were collected with the SSPS at five depths (10, 20, 30, 40, and 50 cm) along nine transects on a 30-m transect spacing for site 1 and four transects on a 20-m transect spacing for site 2. The nominal operating speed of the tractor-mounted SSPS was 1.5 m s^{-1}, selected based on results of soil bin tests (Chung, 2004). An additional four transects (test transects) of data were collected with the SSPS in the opposite direction of travel and parallel to the first set of transects (reference transects) at site 2 to evaluate repeatability of the PSSI measurements. Distances between the reference and test transects were less than 4 m, but no closer than 1 m. Positional information was collected using a DGPS receiver with an accuracy of 1 m or better. The repeatability of soil strength measurements with the SSPS was evaluated by comparing PSSI measurements obtained from the test transects at site 2 with those from the corresponding reference transects. Fifty-two locations spaced 30 m apart along the transects were selected and 4-m averaged PSSIs were obtained for this evaluation. Additional details of the experimental design and data analysis are given in Chung (2004).

Results and Discussion

1. Laboratory Tests and Calibration

An example of the output signal for a static loading and the corresponding histogram are shown in fig. 3. Expressed as DN, the mean of the signal was 110.9±0.1 (95% confidence interval) and the range was 9. The Kolmogorov -Smirnov statistic was 0.164 (n=1995, α<0.01), indicating a normal distribution. Similar results were obtained for the other load cell-amplifier combinations. The range and standard deviation were calculated from each output dataset

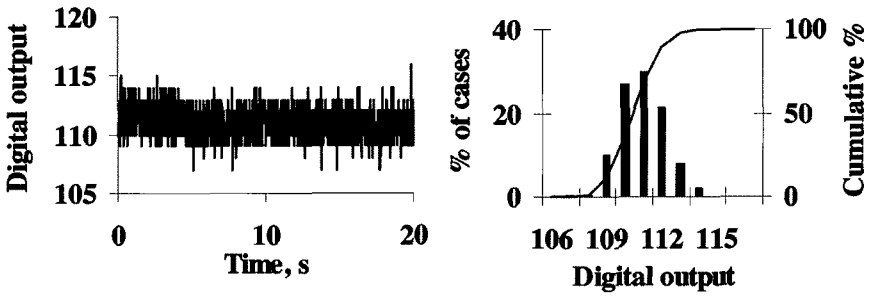

Fig. 3 An example of the output signal for a static loading (left) and the corresponding histogram (right).

collected for the different data acquisition channels and loadings. With a 95% confidence, the means of the ranges and standard deviations were 10.82±0.29 DN and 1.44± 0.04 DN, respectively. From equation (2), the corresponding PSSI statistics were calculated as 0.065±0.002 MPa and 0.009±0.0002 MPa, respectively. This verified that the load cells and data acquisition system were capable of recording reliable, low-noise signals in a static laboratory setting.

Fig. 4 shows the linear response of the load cell/amplifier combination to the applied forces. The slope of the linear regression provided a calibration coefficient to relate the digital output of the system to sensor force (or soil strength). When all data were combined into a single regression (y-intercept=0, α=0.05), the empirical coefficient was the same as the theoretical coefficient given by equation 1. Although this overall slope coefficient differed by as much as 3% from individual amplifier slopes, we judged that the ability to interchange components for troubleshooting or replacement justified the potential decrease in accuracy. Therefore, the theoretical coefficient of 2.17×10^{-3} was used to convert digital outputs (DN) to force measurements (kN), as shown in equation 1.

2. Processing and Mapping Field PSSI Data

Field PSSI measurements showed variations in soil strength at different within-field locations as well as at different tip depths. The field PSSI data contained both high frequency (short-scale) components and underlying low frequency (long-scale) components (fig. 5). High frequency components are often due to measurement system noise and/or micro-variability over small distances. Although it would be important to retain these high- frequency data for some analyses, in this study we averaged the PSSI data to obtain more reliable measurements. Variogram analysis identified two ranges of spatial dependence for both sites, one at distances between 4 and 6 m due to the variability within transects and the other at a distance similar to the transect spacing (Chung, 2004). Based on this analysis, we selected 4 m as the distance over which to average PSSI within transects. About 27 data points were used to calculate each 4-m averaged PSSI value for further analysis, considering the approximately 1.5-m s^{-1} operating speed and 10-Hz sampling rate. This averaging window size (27 points or 4 m) was similar to that used by Lui et al. (1996), who averaged 40 data points over 3 m to obtain a reliable local draft value for a 16-mm-wide shank.

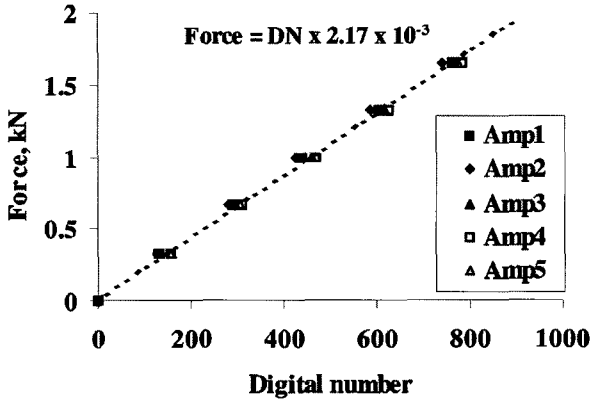

Fig. 4 Relationship of applied static force to digital number (DN) in the load cell calibration tests.

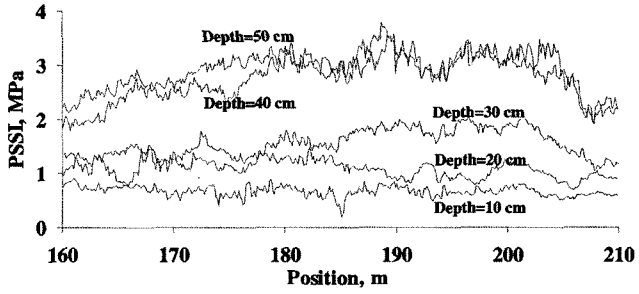

Fig. 5 An example of typical field PSSI measurements at the five tip depths.

As an optimum grid size for PSSI mapping, we selected an intermediate value of the first and second variogram ranges, or 10 m. For Veris-deep EC_a, we selected a 5-m grid size for mapping, since the EC_a variograms showed a range of approximately 5 m for both sites. Fig. 6 shows the resulting kriged maps of PSSI at the five sensing depths and Veris-deep EC_a for sites 1 (top) and 2 (bottom). Compared with the EC_a maps, PSSI maps exhibited coarser spatial patterns due to the greater transect spacings used in data collection. Patterns in the PSSI maps for site 1 were elongated in the north-south direction, an artifact of the difference between the transect spacing (30 m) and the along-transect data spacing (4 m).

Overall, soil strength was higher in areas of lower EC_a, corresponding to lower soil clay fractions and/or lower soil water content. A similar pattern was seen at all depths, but the degree of correspondence between the PSSI and EC_a maps was somewhat different for different depths. For example, in site 1, areas with higher EC_a levels visually corresponded to lower PSSI areas better at the 40-cm depth than at other depths. The overall pattern of higher PSSIs in low EC_a areas, and the different degrees of similarity between PSSI and EC_a maps at different depths were also found in site 2.

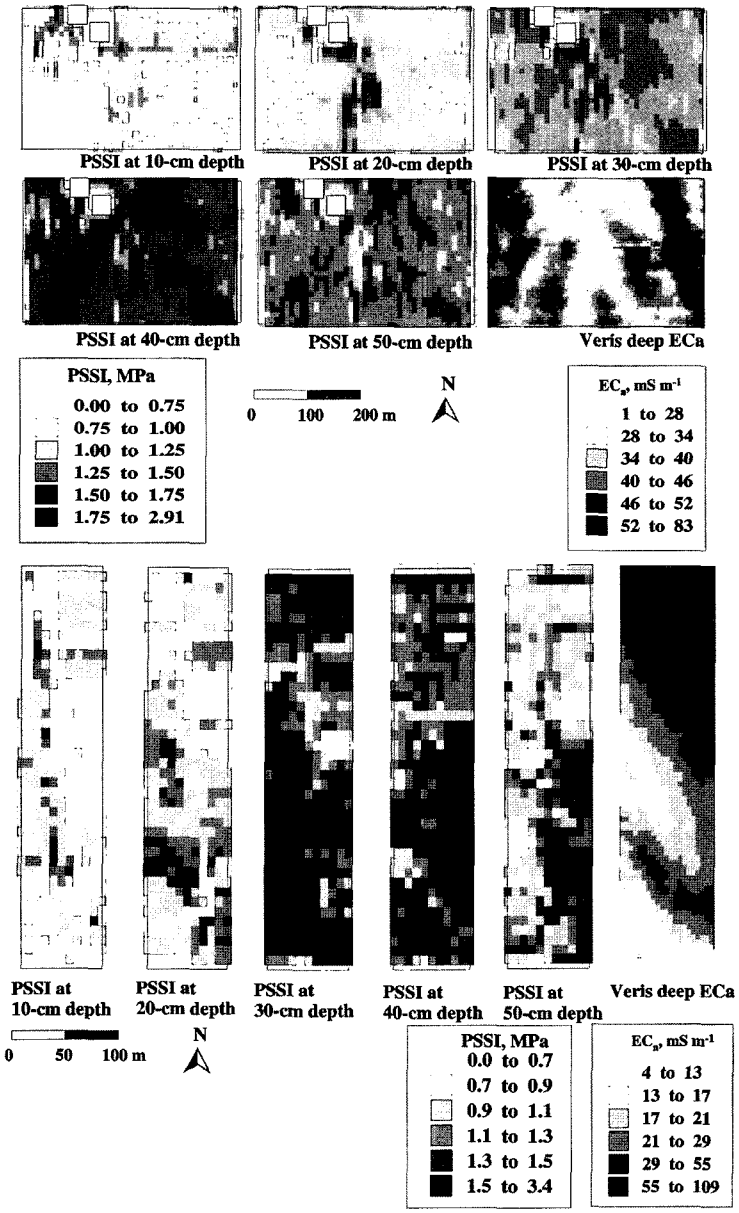

Fig. 6 Kriged maps of PSSI (10-m×10-m grid) at the five sensing depths and Veris-deep EC_a (5-m×5-m grid) for site 1 (top) and site 2 (bottom). White squares in PSSI maps for site 1 are areas of missing data due to incomplete transects.

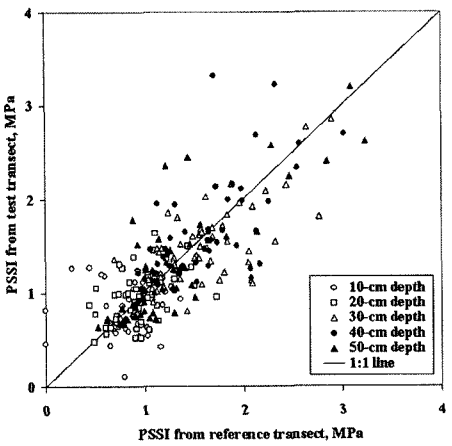

Fig. 7 Comparison of PSSIs from the reference and test transects.

PSSI was highest at the 40-cm depth for both sites. Taylor and Gardner (1963) stated that CI readings above 2 MPa could significantly impede root growth. When this criterion was applied to the 40-cm depth PSSI maps, cells where PSSI was greater than 2 MPa were 4.9% and 15.8 % of the total number of cells for sites 1 and 2, respectively. Based on this criterion and data, soil strength in most areas of these two fields should not be limiting to root growth.

3. Repeatability of Soil Strength Sensing

Fig. 5 shows results of the PSSI repeatability tests in site 2. The 4-m averaged PSSI values from the test transects were linearly related to those from the reference transects, with the data fairly evenly distributed around the 1:1 line. A paired t-test analysis showed that mean PSSI values of the test and reference transects were not significantly different (P=0.36). Considering the inherent soil strength variability present even at small scales, these results led us to conclude that PSSI measurements were repeatable and stable.

Conclusions

A soil strength profile sensor was developed and its performance was evaluated through laboratory and field tests. The SSPS used 5 prismatic sensing tips to measure soil strength at 5 depths up to 50 cm. Laboratory tests for load cell calibration showed a significant (α=0.05) linear response of the system to the applied forces, and the coefficient to convert digital output (DN) to force measurements (kN) was 2.17×10^{-3}. Maps created with SSPS data showed spatial and vertical variability in soil strength. Depth to the restrictive layer was different for different field locations, and only 5 to 16% of the field areas were judged to be highly compacted. Comparison of PSSI field data collected on adjacent, parallel transects conformed that mean PSSI values of the two data sets were not statistically different, and that PSSI measurements were repeatable and stable. Further studies may include testing the SSPS in various field conditions and the use of PSSI data for control of variable tillage operations.

References

Adamchuk, V. I., M. T. Morgan, and H. Sumali. 2001. Application of a strain gauge array to estimate soil mechanical impedance on-the-go. Trans. ASAE 44(6):1377 -1383.

Alihamsyah, T., E. G. Humphries, and C. G. Bowers, Jr. 1990. A technique for horizontal measurement of soil mechanical impedance. Trans. ASAE 33(1):73-77.

Andrade, P., U. Rosa, S. K. Upadhyaya, B. M. Jenkins, J. Aguera, and M. Josiah. 2001. Soil profile force measurements using an instrumented tine. ASAE Paper No. 01-1060. St. Joseph, Mich.:ASAE.

ASAE Standards. 2003a. S313.3. Soil cone penetrometer. St. Joseph, Mich.:ASAE.

ASAE Standards. 2003b. EP542. Procedures for using and reporting data obtained with the soil cone penetrometer. St. Joseph, Mich.:ASAE.

Barber, S. A. 1984. Nutrient uptake by plant roots growing in soil. In Soil Nutrient Bio-availability: A Mechanistic Approach, ch. 4. New York, N.Y.: John Wiley & Sons, Inc.

Busscher, W. J., R. E. Sojka, and C. W. Doty. 1986. Residual effects of tillage on coastal plain soil strength. Soil Sci. 141(2):144-148.

Canarache, A. 1991. Factors and indices regarding excessive compactness of agricultural soils. Soil Tillage Res. 19:145-164.

Chukwu, E., and C. G. Bowers. 2005. Instantaneous multiple -depth soil mechanical impedance sensing from a moving vehicle. Trans. ASAE 48(3):885-894.

Chung, S. O. 2004. On-the-go soil strength profile sensor. PhD Dissertation. Columbia, Mo.:University of Missouri.

Chung, S. O., and K. A. Sudduth. 2003. Modeling soil failure caused by prismatic and conical tools. ASAE Paper No. 031028. St. Joseph, Mich:ASAE.

Chung, S. O., and K. A. Sudduth. 2004. Characterization of cone index and tillage draft data to define design parameters for an on-the-go soil strength profile sensor.

Agric. Biosystems Eng. 5(1):10-20.

Guerif, J. 1994. Effects of compaction on soil strength parameters. In Soil Compaction in Crop Production, eds. B. D. Soane and C. Van Ouwerkerk, ch. 9, 191-214. Amsterdam, Netherlands: Elsevier.

Hall, H. E., and R. L. Raper. 2005. Development and concept evaluation of an on-the-go soil strength measurement system. Trans. ASAE 48(2):469-477.

Koolen, A. J., and H. Kuipers. 1983. Agricultural Soil Mechanics. Berlin, Germany: Springer-Verlag.

Lipiec, J., and W. Stepniewski. 1995. Effects of soil compaction and tillage systems on uptake and losses of nutrients. Soil Tillage Res. 35:37-52.

Lui, W., S. K. Upadhyaya, T. Kataoka, and S. Shibusawa. 1996. Development of a texture/soil compaction sensor. In Proceedings of the Third International Conference on Precision Agriculture, eds. P. C. Robert, R. H. Rust and W. E. Larson, 617-630. Madison, Wisc.: ASA, CSSA, and SSSA.

Mulqueen, J., J. V. Stafford, and D. W. Tanner. 1977. Evaluating penetrometers for measuring soil strength. J. Terramechanics 14(3):137-151.

Sojka, R. E., W. J. Busscher, and G. A. Lehrsch. 2001. In situ strength, bulk density, and water content relationships of a Durinodic Xeric Haplocalcip soil. Soil Sci. 166(8):520-529.

Sudduth, K. A., N. R. Kitchen, G. A. Bollero, D. G. Bullock, and W. J. Wiebold. 2003. Comparison of electromagnetic induction and direct sensing of soil electrical conductivity. Agron. J. 95(3):472-482.

Taylor, H. M., and H. R. Gardner. 1963. Penetration of cotton seedling taproots as influenced by bulk density, moisture content, and strength of soil. Soil Science 96(3):153-156.

Van Bergeijk, J., D. Goense, and L. Speelman. 2001. Soil tillage resistance as tool to map soil type differences. J. Agric. Eng. Res. 79(4):371-387.

Voorhees, W. B., D. A. Farrell, and W. E. Larson. 1975. Soil strength and aeration effects on root elongation. Proc. Soil Sci. Soc. America 39:948-953.